

Mudbank regime off the Kerala coast during monsoon and non-monsoon seasons

R TATAVARTI*, A C NARAYANA#, P MANOJ KUMAR# and SHYAM CHAND#

**Naval Physical and Oceanographic Laboratory, Defence R & D Organization,
Thrikkakara, Cochin 682 021, India*

#*Department of Marine Geology & Geophysics, School of Marine Sciences, Cochin University of Science & Technology, Lake Side Campus, Fine Arts Avenue, Cochin 682 016, India*

Field experiments conducted in the nearshore ocean to understand the dynamics of mudbank off Kerala, south-west coast of India, are highlighted. Real time monitoring of the nearshore ocean off Purakkad, Kerala was accomplished using pressure transducers for nearshore surface wave measurements, and current sensors for nearshore velocity measurements. Comprehensive information on the spatial structure of mudbank was obtained from aerial surveys. Extensive data collected on surface waves and currents in the nearshore ocean, indicate that the infra-gravity (IG) waves (leaky modes and trapped edge wave modes), and far infra-gravity (FIG) waves coupled with strong shoreline reflections and undertow play an important role in the dynamics associated with the mudbanks off Kerala during the monsoon season. During the non-monsoon season evidence for progressive edge waves in the infragravity frequency band, an energetic gravity wave band and a strong undertow with weak reflections was observed.

1. Background

Mudbanks are calm regions of nearshore sea water devoid of any significant wave action due to very high concentrations of sediments in suspension. Mudbanks are unique and occur at only a few locations in the nearshore waters of the world oceans. Along the Indian coasts they are known to occur on the south-west coast especially off Purakkad in Kerala. The Kerala mudbanks *generally* become more prominent with the onset of south-west monsoon (i.e., in the month of June), and less prominent with the withdrawal of the south-west monsoon season. The mudbank appearing off Purakkad, Kerala has socio-economic implications as

- it is known for its very high biological productivity (see Damodaran 1973; Gopinathan and Qasim 1974; Nair *et al* 1984; Rao *et al* 1984; Thompson 1986 for review) and,
- it prevents the otherwise rampant sea erosion (Kurup 1977; Silas 1984; Nair 1985) during the

south-west monsoon season along the Kerala coast (S.W. coast of India). Although a number of studies were made on the formation, sustenance and disappearance of the mudbanks off Kerala, the phenomena still remains an enigma (see Nair 1976; Wells and Coleman 1981; Silas 1984; Wells and Kemp 1986; Froidefond *et al* 1988; Faas 1991, 1992; Mehta and Jiang 1993; Mathew *et al* 1995; Mathew and Baba 1995; Faas 1995; for review).

Of late, coastal and ocean engineers believe that once the dynamics of mudbanks are understood (i.e., *why* and *how* these nearshore oceanic processes occur and sustain before disappearing), the knowledge can be applied for preventing coastal erosion (Hands 1990; McLellan *et al* 1990; Mehta and Jiang 1993) and increasing the productivity of the nearshore oceans.

Earlier studies on Kerala mudbanks covered basically their hydrographic features and physical processes involved in their formation, but did not essentially encompass real time nearshore wave monitoring. Recently Mathew (1992) attempted to explain

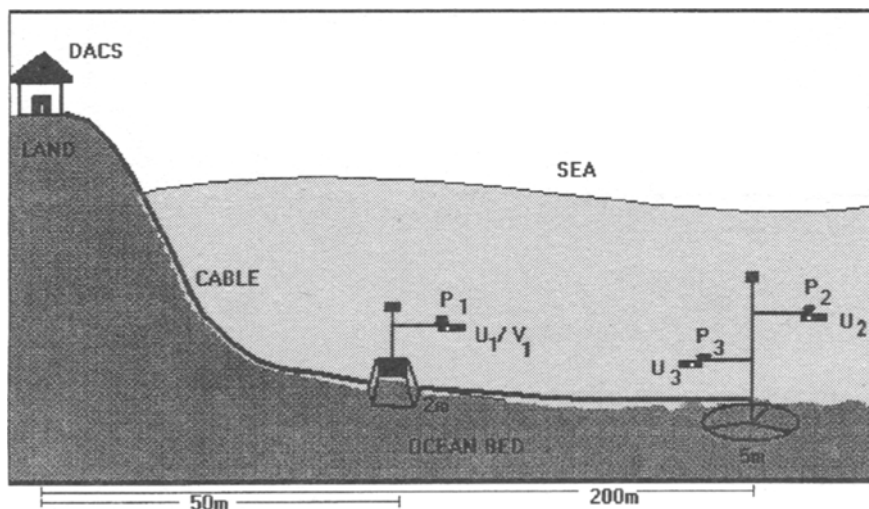
Keywords. Mudbanks; Kerala coast; edge waves; infragravity waves; far infragravity waves; currents; undertow; reflections.

the formation, sustenance and dissipation of mudbanks in terms of measured nearshore wave conditions and sediment characteristics. The study, however, remains incomplete as a number of important parameters could not be monitored in the field. Moreover, a critical examination of nearshore wave spectral figures from Mathew (1992), points out the inability of the wave measuring instruments to monitor frequencies less than 0.05 Hz, which have been known to be very important in the nearshore region. Mathew (1992) also hypothesized with the help of what is termed as a *conceptual model*, the mechanism responsible for the formation, maintenance and dissipation of mudbanks off Allepey. The significant limitation in Mathew's (1992) *model* is that, the role of undertow or mean currents in the offshore direction is completely neglected. Recent publications on mudbanks of the southwest coast of India, by Mathew *et al* (1995); Mathew and Baba (1995); suggest a conceptual model for the formation, sustenance and dissipation of mudbanks based on sparse surface wave data from two spatially separated locations in the cross-shore direction. As the nearshore currents were not monitored during their study, Mathew and Baba's (1995) conceptual model, which strongly relies on presumed current patterns, carries little scientific evidence. Field investigations on various beaches, by Tatavarti and Bowen (1989); Greenwood and Osborne (1990); Putrevu and Svendsen (1993); and others, have conclusively established the significant role played by undertow in the nearshore region in moving the sediments. Mehta and Jiang (1993) calculated the wave attenuations over nearshore underwater mudbanks and mudberms based on a finite amplitude wave-mud interaction (2-D) model and compared them with measurements made off Allepey mudbank by Mathew (1992). Mehta and Jiang's (1993) model does not take into consideration the three dimensional

nature of the wave field and the changing rheology of the mud in the spatial and temporal environment. However, they do claim that their simulations were in agreement with measurements ('*within a reasonable degree of accuracy*'), because they believe that, off Allepey a 3-D condition may not have contaminated the data and the sediment was comparatively uniform. Against this background, we present here some of our significant observations of the hydrodynamics (wave and current motions) in a mudbank regime, based on extensive field experiments (monitoring the nearshore waves and currents), and aerial surveys (video recording the entire coastal ocean in and around mudbank), to obtain a comprehensive picture of this unique phenomenon. In this manuscript, we chose to highlight the nearshore wave and current dynamics during two different real world scenarios in the mudbank regime, i.e., during non-monsoon and monsoon meteorological conditions of the local environment.

2. Field experiments

Major field experiments were conducted in three phases, two during the peak of the S.W. monsoon season (June and August 1995) and one during the non-monsoon season (May 1997); by deploying pressure transducers (for monitoring wave elevations) and current meters (for monitoring nearshore ocean currents), off Purakkad, Kerala, in the nearshore waters of the Arabian Sea. The three phases of the field experiments were carried out to ensure that we record nearshore wave and current data in different spatial and temporal domains, during calm and stormy sea conditions. Both pressure transducers and current meters were indigenously designed and fabricated. The pressure transducers were inductance type, and the current meters were bi-directional drag force



MUDBANK '95 & '97 - SCHEMATIC OF FIELD EXPERIMENTAL SETUP

Figure 1. Section view of the sensor deployment on under water platforms for data acquisition.

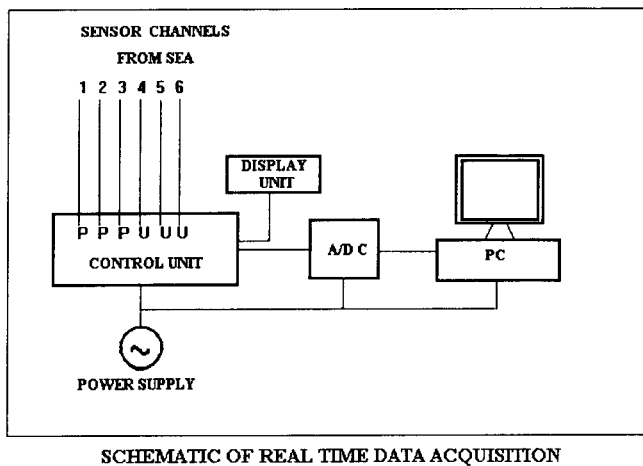


Figure 2. Schematic of real time data acquisition set up.

sensors, designed to record the current speeds in any aligned direction (i.e., depending on the orientation of the current meter either the cross-shore component or the alongshore component of the nearshore velocity may be monitored). Sensor calibrations were performed in a towing tank with random wave generation facility. Extensive intercomparisons with other available standard instrumentation were performed in order to assess the performance of the sensors. During the calibration and intercomparison experiments, checks for the robustness and sensitivity of the sensors were made. The response time of the pressure sensors and the current meters was found to be approximately 0.2 sec. The frequency response of the pressure sensor was near unity between 0 and 2 Hz, while the frequency response of the current sensor was near unity between 0 and 5 Hz. The sensors were deployed in the ocean by fixing them on stable underwater platforms, sitting on the ocean bed (figure 1). The sensor locations were designed to capture the horizontal and vertical structure of the nearshore wave and current regime. Underwater coaxial cables were used to transmit signals between sensors in the ocean and the shore based control unit. Figure 2 shows a schematic of the real time data acquisition set up. The analogue signals from the control unit were piped through an A/D card (analogue to digital conversion) into a personal computer in order to store real time digital data. The frequency and duration of data sampling was controlled by the shore based computer. Data was sampled at 2 Hz. Aerial surveys of the mudbank and its surroundings were conducted during all the three phases of the major field experiments from a helicopter, to obtain a comprehensive picture in the spatial domain. The aerial survey was timed to coincide with our field experiments in the sea. During the aerial surveys, video recording was carried out using a CCD camera (*Sony Betacam*, Japan), on board the helicopter. Position fixing on board the helicopter, during aerial surveys and on a small vessel during bathymetry survey, was accomplished by using a portable

Global Positioning System (*Trimble GPS*, USA) whose accuracy was ± 15 m. Bathymetry surveys were conducted using an echo sounder (*Furuno*, Japan). During the three phases of experiments, more than 120 surface sediment samples were collected using the Vanveen grab sampler from different offshore locations in the mudbank. Beach profiling was carried out at 38 locations spatially separated by 500 m along the coast, every month for two years and also during the major field experiments. Beach surveys were carried out using a Theodolite and a graduated rod, up to 1 m water depth from local bench mark positions along the coastline. The physical properties of mudbank sediments based on our field investigations have been reported elsewhere (Manoj Kumar *et al* 1998) and are not being discussed here as the topic does not fit into the scope of the present study.

3. Observations

3.1 Monsoon season

Based on the recorded footage from our aerial surveys, the schematic picture of the mudbank and its peripheries was drawn and is shown in figure 3. Figure 3(a) shows the schematic of the sensor deployment (planar view) *vis-a-vis* the mudbank location during phases I and II, while figure 3(b) shows the schematic of sensor deployment (planar view) *vis-a-vis* mudbank location during phase III of the field experiments. During the rough monsoon season, the periphery of the mudbank extends to about 10 km seawards from the shoreline and stretches for about 15 km alongshore. The calm region is observed to be separated from the rough sea (significant wave height, H_s ; 2.5 m) by a transition zone where low frequency infra-gravity waves were observed to be dominant. The sediment concentration levels were the highest in the calm zone decreasing progressively towards the rough sea. The calm zone was observed to be buffeted by a straight shoreline, while the transition zone by shoreline cusps (figure 3a). During our observations the mudbank region was noticed to wax and wane with changing wind conditions. Strong onshore winds were responsible for the contraction of the mudbank region. At the northern and southern boundaries of the mudbank slowly propagating solitary waves were observed all the time. During the monsoonal period, the mudbank region and its surrounding sea was observed to have significantly strong shoreline reflections of waves. Surging and spilling breakers were observed in the transition zone, while plunging breakers were observed in the rough zone. The surf zone in the transition zone inside the mudbank was narrow (approx. 10 m), while that in the rough sea was wide (approx. 50 m). During our daily inspection of sensors at low tides, we have felt very strong alongshore and cross-shore currents with a relatively long periodicity (low frequency). The sea

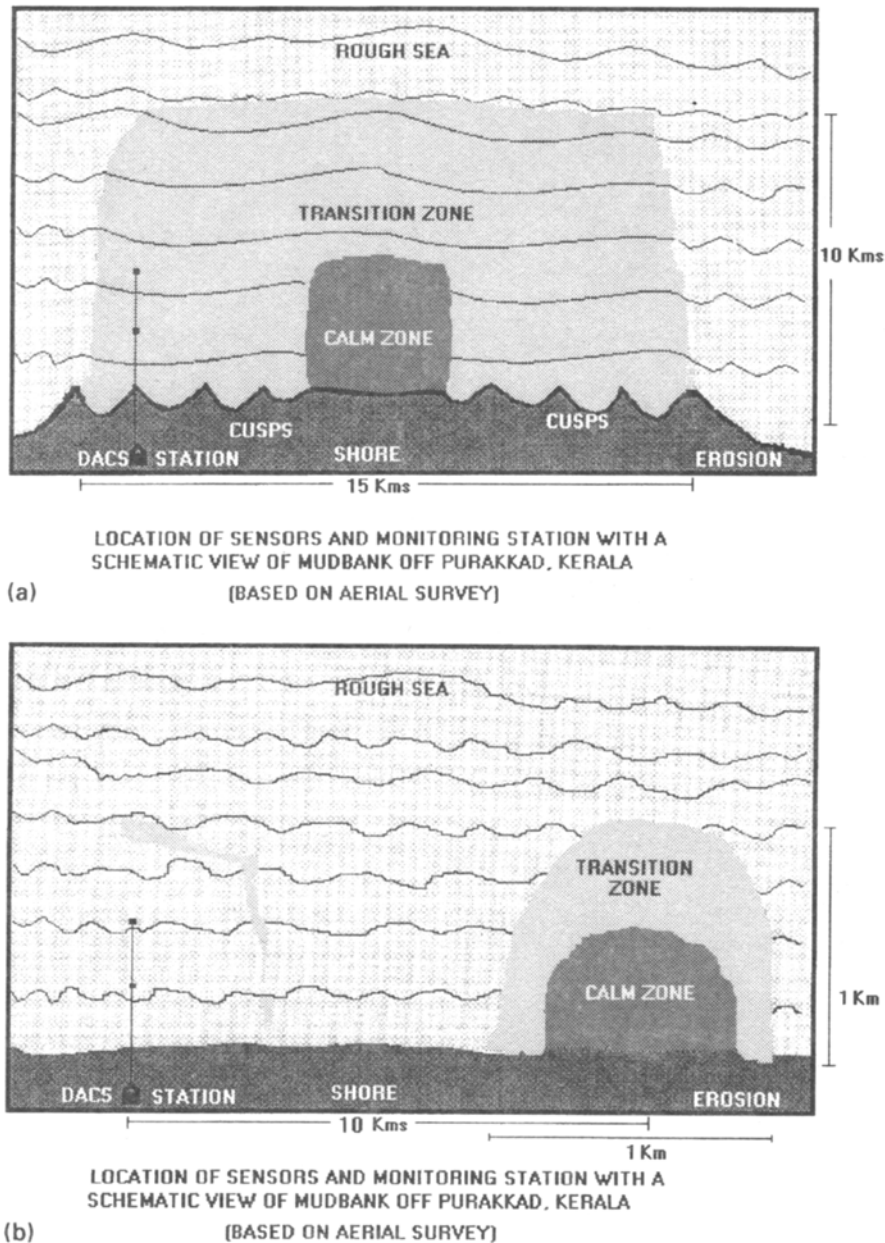


Figure 3. Schematic view of mudbank off Purakkad, Kerala, based on aerial survey during (a) monsoon and (b) non-monsoon seasons.

bed was observed to have sinusoidal undulations (with vertical amplitudes of 5–10 cm and horizontal spacing of 1–2 m), slightly oblique to the shoreline. The beach cusp spacing in the transition zone, where our instruments were deployed, varied from 8.5 m to 26.5 m with average vertical amplitudes of 0.5 m.

3.2 Non-monsoon season

During the non-monsoonal period, the spatial extents and the suspended sediment concentrations were observed to gradually become smaller (figure 3b). From our field experiments we noticed that the mudbank which existed as a small patch in March 1995, reactivated with the onset of monsoon, gradually expanded and reached its maximum extension

(figure 3a) in October – November 1995. The expansion of the mudbank was towards south during the S.W. monsoon period. During the non-monsoonal season the shoreline was generally straight, devoid of any cuspy features. Gravity waves were predominant and observed to be characteristically breaking slightly offshore (approx. 200 m offshore). Wave reflections were observed to be rather weak. The significant wave heights during our observations were of the order of 1.5–2.5 m. Waves were predominantly observed to be approaching from northwest. Whenever, the wind activity was strong, well formed cusps with 15–20 m alongshore spacing and heights of 0.5–0.7 m were observed. During our periodic inspection of sensors, strong undertow and longshore currents were observed, whenever wind and wave activity were stronger.

The surf zone comprised of plunging and collapsing breakers, with a surf zone width around 10–20 m.

4. Sediment characteristics and their probable source

Based on field observations during non-monsoon and monsoon seasons, the surface sediment (on the ocean bed) particle sizes, their spatial distribution and their geotechnical characteristics in the Ambalapuzha-Purakkad mudbank were studied and the details were reported by us elsewhere (Manoj Kumar *et al* 1998). The study revealed that the sediments in the mudbank are clayey silts in both seasons. The magnitude of the fine silt and clay contents, blanketing the ocean bed were however, observed to be more in the pre-monsoon season indicating the possibility of fine silt and clay going into suspension during the monsoon season. Geotechnical properties of surface sediments revealed that they are highly plastic with high liquid limits. It was also observed that the high organic matter in fine sediments plays an important role in the behaviour of the physical characteristics of sediments and their suspension. As it was observed that the mudbank sediments exhibit almost similar physical properties in both monsoon and non-monsoon seasons, the earlier reported suggestions by various other authors, regarding the transportation of fine sediments, from offshore to nearshore region during monsoon and vice versa during non-monsoon seasons, may not be valid. Our observations suggest that only re-suspension and re-deposition processes may be the important factor in mudbank dynamics.

5. Data for analysis

Although extensive data collection was carried out during the three phases (at 2 Hz sampling, with continuous data recording for 5, 10 and 5 *days* durations) of the field experiment, only representative data sets from

- (a) the first phase of our experiments, when the S.W. monsoon was active *but* calm sea conditions persisted (specifically data recorded on the night of June 24th, 1995 when light to moderate winds during low tide prevailed),
- (b) the second phase of our experiments, when the S.W. monsoon was active and stormy sea conditions persisted (specifically on August 31st, and September 1st, 1995 when strong winds during rising tide prevailed), and
- (c) the third phase of our experiments when S.W. monsoon was not yet set *but* stormy sea conditions persisted (specifically data recorded on the night of May 9th, 1997 when strong winds prevailed during low tide), were presented in this paper to

demonstrate the varying nearshore wave and current dynamics in the mudbank regime during changing sea conditions in the monsoonal and non-monsoonal seasons respectively. The primary reasons for choosing this specific data set were that

- on June 24th, 1995, although calm meteorological conditions prevailed, strong alongshore currents towards north were noticed during our periodic inspection of sensors,
- a very long data set (9 hr duration) was recorded on that night (June 24th, 1995) during which time tide was ebbing,
- on August 28th, 1995 no significant wind activity was observed and the local sea was very calm,
- on August 31st, 1995 very strong winds were observed and the sea was choppy and there was a torrential downpour,
- on September 1st, 1995 very strong winds were observed, no rain was present but the sea became very choppy and the seaward boundary of the mudbank contracted towards the shore, and finally,
- on May 9th, 1997, very strong wind and wave activity was observed during the low tide as a local meteorological disturbance lay centred off the coast of Kerala.

6. Results and discussion

During phase I and phase II of the field experiments the sensor pair ($P1$, $V1/U1$) were collocated on a platform at a height of 1 m from the ocean bed, in 2 m water depth. Sensor pairs ($P2$, $V2/U2$), and ($P3$, $V3/U3$) were deployed in 5 m water depth, fixed on a platform. Sensors ($P2$, $V2/U2$) were collocated at a height of 2 m from the ocean bed, while ($P3$, $V3/U3$) were collocated at a height of 1 m from the ocean bed. The first platform in 2 m water depth was located at an offshore distance of 50 m from the shoreline, while the second platform in 5 m water depth was located at an offshore distance of 200 m from the shoreline. During the phase III of the field experiment however, only one platform (i.e., at 5 m water depth) was deployed with collocated P , U and V sensors at a height of 1 m from the ocean bed and another P sensor at a height of 2 m from the ocean bed. Because of the strong wave activity in the surf zone, during phase III, the first platform could not be deployed with our existing logistic support.

Care was taken while analysing the data sets, not to contaminate the analysis with any existing trends in time series (for instance, mean longshore current and tidal trends). The importance of infragravity wave [$O(10^{-2}$ Hz)] and far infragravity wave [$O(10^{-3}-10^{-2})$ Hz] dynamics in the nearshore waters and their role in the mudbank region was reported earlier (Tatavarti

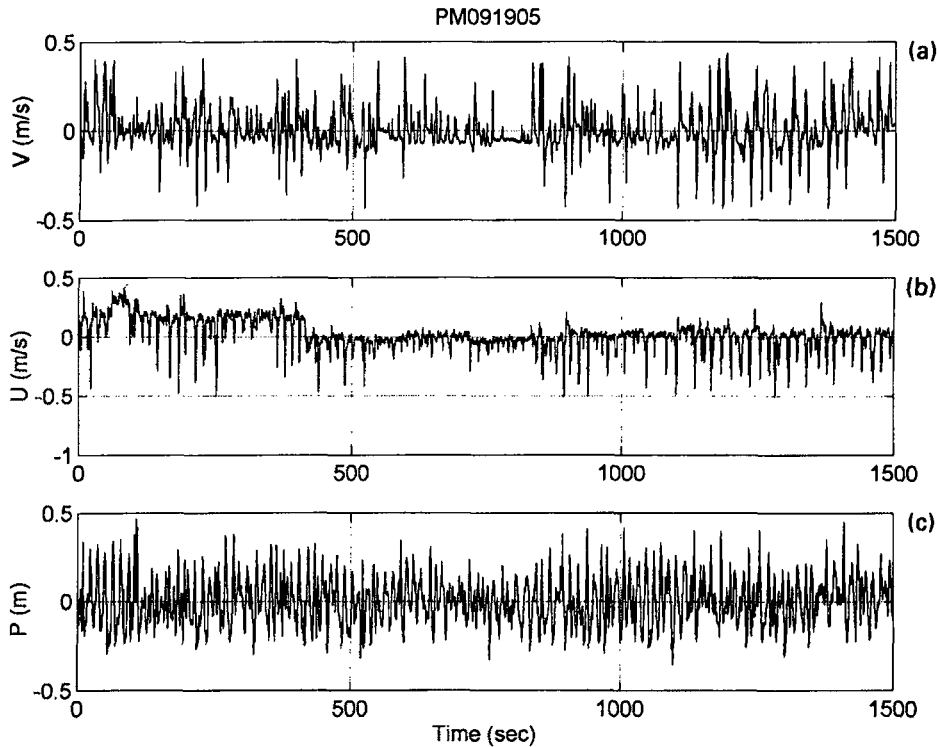


Figure 4. Representative time series of v , u and η from the long data set collected on May 9th, 1997 (non-monsoon season) during ebbing tide and strong wind activity. The time series were demeaned and detrended.

et al 1996). Our first results from phase I of the field experiment, conducted during the monsoon season, clearly indicated that the infragravity (IG) waves (*leaky modes and trapped edge wave modes*) and far infragravity (FIG) waves, coupled with strong reflections and undertow play an important role in the dynamics associated with the mudbanks off Kerala (Tatavarti *et al* 1996).

Typical sections of twenty five minute long raw time series of the alongshore component (v) from V , cross-shore component (u) from U and the surface elevation [$p(\eta)$] from P sensors, based on field observations during the non-monsoon season, are presented in figure 4. As can be seen there are no trends and offsets in the time series to contaminate our spectral computations. Large amplitudes (~ 0.6 m/s), and long period oscillations (~ 1000 sec) are clearly present in the cross-shore component of the velocity (figure 4b). The predominant direction of the cross-shore velocity is seaward. As the sensor is near the bottom of the ocean, the seaward flowing current may be construed as representative of the undertow. Alongshore velocity (figure 4a) also shows similar long-period oscillations but they are less pronounced. The alongshore velocity component shows predominantly gravity wave motions with mean amplitudes of 0.5 m/s. The predominant direction of alongshore velocity is northwards. These features are consistent with the field observation that the predominant wind and waves were approaching from northwest. Oscillations with periodicities of gravity waves are very prominent in

the surface elevation time series record (figure 4c). The variances associated with the time series oscillations of figure 4 are evident in the frequency spectra (figure 5). The spectra shown in this paper were generated from consecutive 4096 sec time series sections. Each section was detrended using a quadratic function (to remove tide) and demeaned before Fourier transformation. Spectral computations were made using a 50% overlap Hanning spectral window having 60 degrees of freedom (*dof*) and a frequency resolution of 0.00048 Hz. Typical spectra of wave elevation (η) from P sensor, cross-shore current (u) from U sensor, and alongshore current (v) from V sensor based on observations *during the non-monsoon season* are shown in figure 5. These spectra were computed from collocated sensors located at a water depth of 5 m and a height of 1 m from the ocean bed. Typical spectra of wave elevation, cross-shore velocity and alongshore velocity based on observations *during the monsoon season* are shown in figure 6. The 95% confidence levels are the same for all spectra and are shown along with the spectra in figures 5 and 6. The most prominent feature in figure 5, i.e., for field observations during the non-monsoon season, is that the spectral energy levels are a maximum in the gravity band for both wave elevation and alongshore velocity, but for the cross-shore velocity the maximum energy lies in the FIG band. This may be an artifact of the pulsating cross-shore mean current. Three features that stand out from figure 6, are:

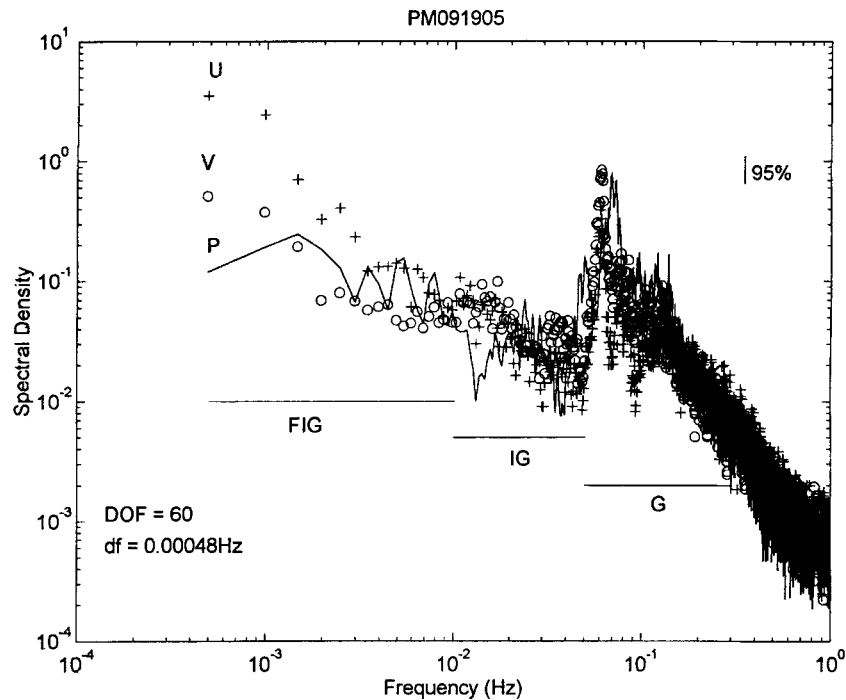


Figure 5. Spectra of v , u and η . The FIG, IG and G bands are marked. Data from V , U and P sensors of phase III of field experiment during non-monsoon season. 95% confidence levels are shown in the upper right corner. DOF = 60, and freq. resolution is 0.000488 Hz.

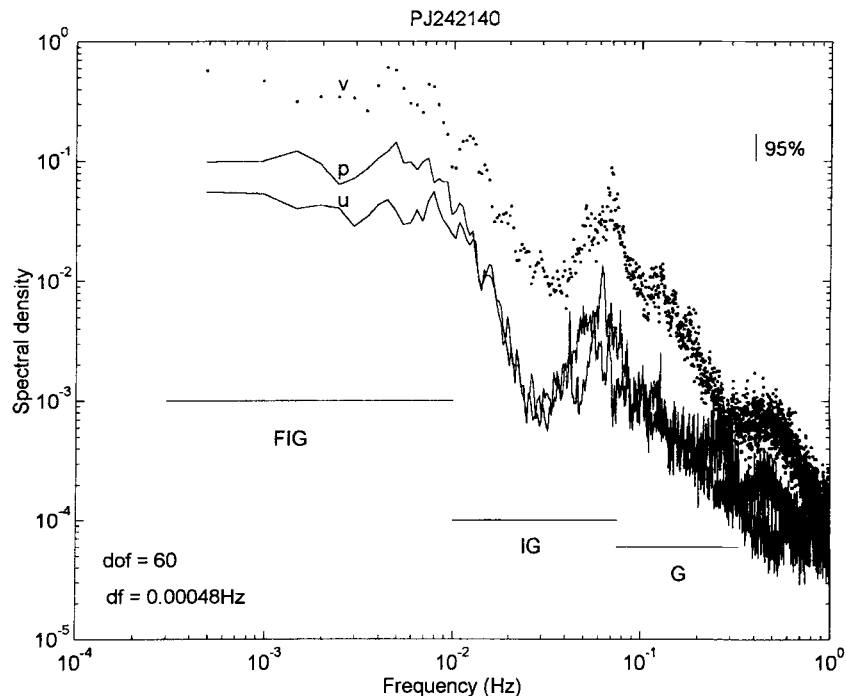


Figure 6. Spectra of v , u and η . The FIG, IG and G bands are marked. Data from $V1$, $U2$ and $P1$ sensors of phase I of field experiment during monsoon season. 95% confidence levels are shown in the upper right corner. DOF = 60, and freq. resolution is 0.000488 Hz.

- the low frequency energies in all spectra are maximum, the far infra-gravity band (10^{-3} – 10^{-2} Hz frequency band) having about two orders of magnitude more energy compared to gravity waves (10^{-1} Hz);
- the alongshore component (v) of the nearshore velocity is an order of magnitude stronger than the cross-shore component (u) in the FIG and IG bands;
- the wind wave frequency band (gravity waves) is least energetic. The features in the IG band (i.e.,

Table 1. *Statistics of wave elevation and currents in mudbank regime.*

Data run/date/time	v/u	η Mean (m)	η Variance (m^2)	u Mean (m/s)	u Variance (m/s)	v Mean (m/s)	v Variance (m^2/s^2)	Remarks
PJ242140 June 24th, 1995 @ 2140 hrs	0.8745	2.6232	0.1007	1.1268 (seaward)	0.0033	0.7716 (northward)	0.0174	Light to moderate winds. Waves approaching from NE. Ebbing tide. Strong reflections, undertow, longshore currents.
PA282330 August 28th 1995 @ 2330 hrs	0.62126	2.9944	0.0285	1.4973 (seaward)	0.0057	0.4291 (northward)	0.0022	No wind. No rain but overcast. Calm sea. Ebbing tide. Strong reflections, undertow, longshore currents.
PA311550 August 31st, 1995 @ 1550 hrs	0.5246	3.4384	0.1659	1.3511 (seaward)	0.0012	-0.6760 (southward)	0.0175	Strong winds. Sea choppy. White caps. Raining. Very low freq. periods. Harmonics. Rising tide. Strong reflections, undertow, longshore currents.
PS012230 September 1st, 1995 @ 2230 hrs	0.77459	3.0875	0.0981	1.504 (seaward)	0.0015	-0.7933 (southward)	0.0009	Monsoonal strong winds. Sea choppy. Seaward boundary of mudbank at 600 m offshore. Rising tide. Strong reflections, undertow, longshore currents.
PM091905 May 9th, 1997 @ 1905 hrs	0.0859	3.3236	0.2097	0.6182 (seaward)	0.0317	-0.5316 (southward)	0.0213	Strong wind activity and predominant wave approach is from NW. Mostly linear dynamics. Ebbing tide. Rough sea conditions. Weak reflections. Non-monsoon conditions.

$\langle v \rangle / \langle u \rangle$ of the spectra in figure 6 along with our observations of shoreline cusps are consistent with edge wave dynamics (i.e., the presence of trapped modes in the infra-gravity frequency band). The fact that the variance in the v component is larger by an order of magnitude compared to that in the u component in the FIG band (figure 6) suggests the role of a strong alongshore current and is consistent with FIG wave dynamics discussed in the preceding sections. Based on data observed during the monsoon season it was earlier established (Tata-varti *et al* 1996) that the cross-shore velocity in the FIG band was larger near the ocean bottom as compared to that in the middle of the water column, indicative of a strong undertow (Putrevu and Svendsen 1993).

Table 1 shows the statistics of wave elevation and currents in a mudbank regime during different seasons under varying local environmental conditions. The data shown in table 1 pertain to collocated sensors at a height of 1 m from the ocean bed in a water depth of approximately 5 m. It is evident from table 1 that during *both* the seasons, under varying environmental conditions, the mean u values, are significantly strong and suggest seawards flowing cross-shore currents, indicative of a strong undertow. Slightly weaker, yet significant, alongshore currents are also observed during both the seasons under varying environmental conditions. The direction of the alongshore currents seems to be influenced predominantly by the incoming wave directions. The significantly large $\langle v \rangle / \langle u \rangle$ ratios for observations during the phase I and II of the field experiment, during the monsoon season, suggests the importance of edge waves in the infragravity frequency band. The smaller $\langle v \rangle / \langle u \rangle$ ratio for observations during the phase III of the field experiment, during the non-monsoon season, suggests the lack of presence of edge wave motions, however, it is important to note that due to the near normal incidence of waves the ratio may be less even in the presence of edge waves because of the low coherency in the infragravity band between v and u . This is consistent with the absence of shoreline cusps during our visual observations during calm conditions and the presence of shoreline cusps during stormy conditions (when near normal wave incidence prevailed). The varying tidal conditions are reflected in the mean wave elevation values, while the varying variance levels of η , u and v indicate the varying environmental conditions. Generally, the stronger the wind and wave activity the larger the variance of these parameters. Another significant observation is that during the monsoon season the wave reflections from the shoreline are strong, whereas, during the non-monsoon season the shoreline reflections are weak. This is consistent with the fact that the waves were observed to be significantly breaking (plunging and collapsing breakers)

during our field experiments in the non-monsoon season compared to the regular swashing to and fro motion during the monsoon season.

A comparison of figures 5 and 6 reveals some of the pertinent differences in hydrodynamics during the monsoon and non-monsoon seasons. While during the monsoon season FIG waves predominate and play a vital role in the nearshore dynamics, during the non-monsoon season the gravity waves are dominant. The alongshore velocity was observed to be stronger than the cross-shore velocity during the monsoon season, while the cross-shore velocity was stronger than the alongshore velocity during the non-monsoon season. In addition during the non-monsoon season the energy levels in the gravity and infragravity bands were observed to be higher than those during the monsoon seasons, while the energy levels for the FIG band was observed to be higher during the monsoon season, than that during the non-monsoon season.

Figure 7 shows the cross-spectral amplitudes, phases and coherences between PU , PV and VU sensor data observed during the non-monsoon season. The upper 95% confidence level for coherence computations is 0.2 and is shown in figure 7 as a horizontal line in the coherence plot. The features evident from figure 7 are

- highest coherence between PU , PV , VU in the gravity band with in-phase relationships between $P-U$, $P-V$ and $V-U$;
- significant high coherence between PU and PV and low, but significant, coherence between VU in the infragravity band with in-phase relations between them; and
- significant coherence between PV , VU in FIG band. The highest coherence was observed between VU and the lowest between PU .

Tables 2 and 3 show the cross-spectral phase relationships between P , U , V parameters with statistically significant coherence levels. Cross-spectral information of the P , U , V sensor data suggests linear dynamics of the gravity band waves during the non-monsoon season and monsoon season. During the monsoon season (mudbank season) it can be seen from table 2 that in the FIG band the highest coherence is between P and U , with P leading U in quadrature. It is also found that in the FIG band P leads V in quadrature while V leads U in quadrature. These results are consistent with the characteristics of FIG waves (Oltman-Shay *et al* 1989). The coherence in the IG band is also significant, but the coherence in the gravity wave band is not significant, except between P and U . In the IG band the highest coherence was found between P , U and U , V pairs of series although the coherence between P , V pair is also significant. It can be noticed from table 2 that in the IG band, P leads U and V in quadrature, while V leads U in phase. These features in the IG band are consistent with the standing edge wave dynamics (Kim and

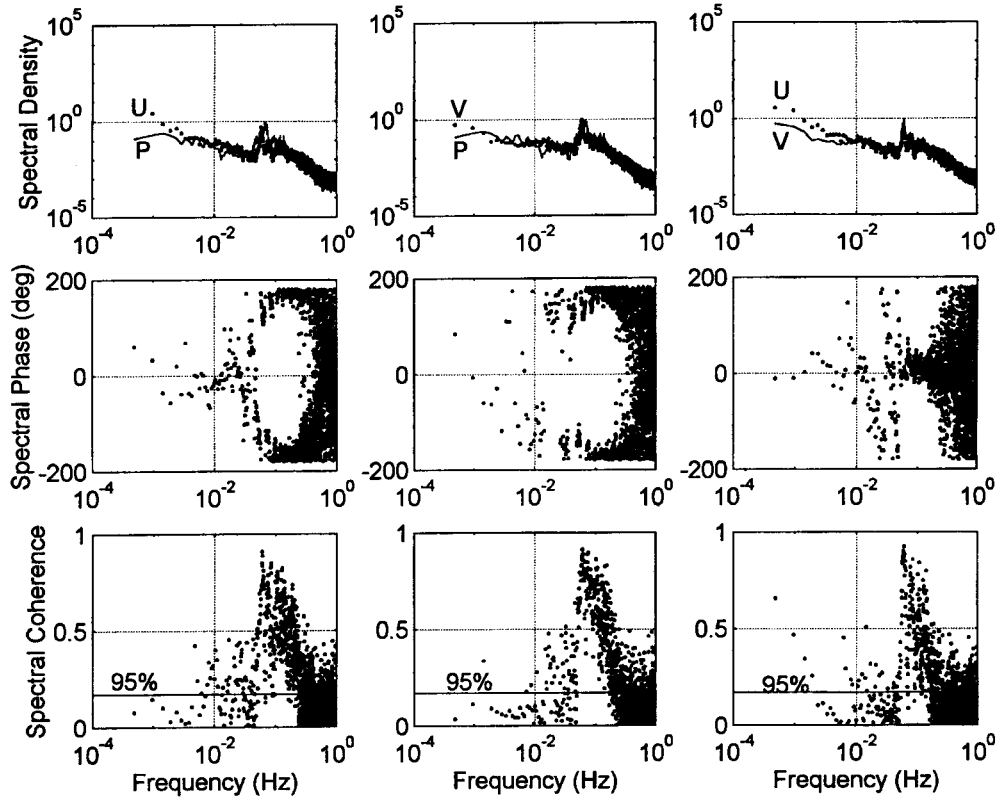


Figure 7. Cross-spectral amplitude, phase and coherence plots for data from PU , PV and UV pairs of sensors of phase III of field experiment during non-monsoon season. Statistics of spectra are the same as those in figure 5. The 95% upper confidence level for coherence is drawn as a horizontal line in the coherence plots.

Table 2. Spectral characteristics in a mudbank region: Monsoon season.

Spectral frequency band	$\eta - u$ Cross-spectral phase	$\eta - v$ Cross-spectral phase	$v - u$ Cross-spectral phase	Remarks
G	in	in	in	<ul style="list-style-type: none"> • no lead/lag between η, u, v. Linear phase between v and u indicative of travel time associated with distance of separation.
IG	out	out	in	<ul style="list-style-type: none"> • η leads u • η leads v • v leads u
FIG	out	out	out	<ul style="list-style-type: none"> • η leads u • η leads v • v leads u

Table 3. Spectral characteristics in a mudbank region: Non-monsoon season.

Spectral frequency band	$\eta - u$ Cross-spectral phase	$\eta - v$ Cross-spectral phase	$v - u$ Cross-spectral phase	Remarks
G	in	in	in	<ul style="list-style-type: none"> • no lead/lag between η, v, u
IG	out	in	out	<ul style="list-style-type: none"> • η leads u • η leads v • u leads v
FIG	out	out	in	<ul style="list-style-type: none"> • η leads u • v leads η • u leads v

Huntley 1985). Naturally occurring frequency dependent shoreline reflections were computed following the noise free technique developed by Tataavarti (1989) and validated by Huntley *et al* (1995) utilizing time series measurements from co-located η and u sensors. Although details of the computations are not being presented here, it was observed that generally the reflections in all frequency bands were significantly high (0.6), the highest being in the lower frequencies (0.8). These strong reflections are consistent with our observations of sea bed undulations (Silvester 1977).

During the non-monsoon season (*non-mudbank season*), in the infragravity frequency band significant coherence between P and U , and P and V was observed with P leading U in quadrature and P leading V in phase. There was low coherence (although significant statistically) between V and U , with U leading V in phase. In the FIG wave band significant coherence between PV and VU was observed, with V leading P in quadrature and U leading V in phase. The coherence level between PU was low with P and U in quadrature, P leading U . These observations do suggest the presence of either standing wave motions or progressive edge waves in the nearshore (Kim and Huntley 1985; Tataavarti 1989). However as our visual observations showed (table 1, PM091905 data run) there was strong wind activity during this observation and weak reflections were noticed. Therefore we infer the presence of progressive edge waves in the infragravity frequency band during these observations. This is again consistent with our observation that shoreline cusps were observed during the non-monsoon phase of field experiments whenever wind activity picked up.

7. Conclusions

Extensive field experiments conducted in the mudbank off Purakkad, Kerala provided a comprehensive picture of the unique phenomenon. The following conclusions are drawn based on the analysis of typical data sets collected at a sampling rate of 2 Hz, during the monsoon and non-monsoon seasons. During our observations in the monsoon season, our analysis established that far infra-gravity (FIG) wave energy is about two orders of magnitude larger than that of gravity waves, while during the non-monsoon season the FIG waves exhibited low energy levels.

During the monsoon season a strong back shear presumably makes the longshore current unstable to a wide range of small perturbations, which in turn is responsible for the FIG waves. The lower energy levels in the FIG wave band during the non-monsoon season (when wave breaking was more pronounced and surf zone width was larger), are consistent with the studies of Putrevu and Svendsen (1992) and Dodd *et al* (1992), which showed that the number of possible unstable

modes of shear instabilities and their corresponding growth rate are reduced if dissipation due to bottom friction and eddy viscosity is increased. Evidence of edge waves in the infra-gravity band and a strong undertow was demonstrated during both monsoon and non-monsoon seasons. During the monsoon season our observations suggested the presence of standing edge wave motions, while during the non-monsoon season our observations suggested the presence of progressive edge wave motions in the mudbank regime. This is presumably the first study to establish the evidence of FIG waves, edge waves and undertow in the mudbank region. The demonstration of FIG waves supports the suggestion of Bowen and Holman (1989), that FIG waves may be a common feature in the nearshore oceans in the presence of longshore currents.

During the monsoon season the computed shoreline reflections were observed to be very high, with approximately 80% of the low frequency waves being reflective. Even gravity waves were found to be strongly reflective (mean reflection coefficient of 0.6). During the non-monsoon season we observed that the gravity wave band is highly energetic with waves breaking significantly before reaching the shore. The shoreline reflections as can be expected in such scenarios were found to be very weak.

Based on our field observations and detailed analysis we now report that the sediments lying on the ocean bed, as a thick blanket in the nearshore region, get disturbed during the monsoon season, because of the larger and stronger waves and therefore are triggered into suspension mode. Later, as the wave energy increases the low frequencies start becoming prominent and become stronger. As these low frequency motions are three dimensional, they carry the suspensions laterally also, thereby resulting in an increase of spatial (on-offshore and alongshore) extents of mudbanks during the monsoon. Once wave heights increase (stronger monsoonal forcing) the breaker zone is shifted seaward, hence suspension events start from a farther seaward location. Also, as wave height increases we have observed that the magnitude of undertow increases; which forces fine sediments from the nearshore to seaward locations. These offshore transported material causes increased suspension events in the seaward location.

Acknowledgements

This study was sponsored by SERC, Department of Science and Technology, New Delhi under the project 'Sediment dynamics and hydrodynamics of mudbanks off Kerala' (ESS/CA/A1-14/93). Dr. K R Gupta, DST is gratefully thanked for his encouragement and invaluable assistance. Tataavarti thanks the Director, NPOL for encouragement. We are thankful to Dr. M Ravisankar, our colleague, for his valuable help

and support during our field experiments. We gratefully acknowledge the logistic support and encouragement provided by Dr. Shanmugam and Shri Gopalakrishnan and family, Purakkad during the field experiments.

References

- Bowen A J and Holman R A 1989 Shear instabilities of the mean longshore current: (1) Theory; *J. Geophys. Res.* **94(C12)** 18023–18030
- Damodaran R 1973 Studies on the benthos of the mudbanks of the Kerala coast; *Bull. Dept. Mar. Sci., Univ. of Cochin* **VI** 1–126
- Dodd N, Oltman-Shay J and Thomson E B 1992 Shear instabilities in the longshore current: A comparison of observations and theory; *J. Phys. Ocean.* **22(1)** 62–82
- Faas R W 1991 Rheological boundaries of mud: Where are the limits?; *Geo. Mar. Lett.* **11** 143–146
- Faas R W 1992 Rheological characteristics of Allepey mud and their role in the formation and maintenance of mudbanks on the Kerala coast of south west of India; *EOS Trans. AGU* **73(43)** 290
- Faas R W 1995 Rheological characteristics of Allepey mud and their role in the formation and maintenance of mudbanks on the Kerala coast of south west of India; *J. Coast. Res.* **11** 188–193
- Froidefond J M, Pujos M and Andre X 1988 Migration of mudbanks and changing coastline in French Guiana; *Mar. Geol.* **84** 19–30
- Gopinathan C P and Qasim S Z 1974 Mudbanks of Kerala, their formation and characteristics; *India J. Mar. Sci.* **3** 105–114
- Greenwood B and Osborne P D 1990 Vertical and horizontal structure in cross-shore flows: An example of undertow and wave setup on a barred beach; *Coast. Engg.* **14** 543–580
- Hands E G 1990 Results of monitoring the disposal berm at Sand Island, Alabama, Report 1: Construction and first year's response Tech. Rep. DRP-90-2, U.S. Army Eng. Waterways Expt. Sta, Vicksburg, Miss, 59 pp
- Huntley D A, Simmonds D and Tatavarti R 1995 On the measurement of coastal reflection using colocated elevation and current sensors; *Coastal Engg.* ASCE 57–68
- Kim C S and Huntley D A 1985 On time delays in the nearshore zone between onshore and longshore currents at incident wave frequencies; *J. Geophys. Res.* **91(C3)** 3967–3978
- Kurup P G 1977 Studies on the physical aspects of mudbanks along the Kerala coast with special references to Purakkad mudbank; *Bull. Dept. Mar. Sci. Univ. Cochin* **VIII** 1–72
- Manoj Kumar P, Narayana A C and Tatavarti R 1998 Mudbank Dynamics: Physical properties of sediments; *J. Geol. Soc. India* **51** 793–798
- Mathew J 1992 Wave-mud interactions in mudbanks. Ph.D Thesis, Cochin Univ. of Science and Technology, Cochin, India, 139 pp
- Mathew J, Baba M and Kurien N P 1995 Mudbanks of SW coast of India I: Wave characteristics; *J. Coast. Res.* **11** 168–178
- Mathew J and Baba M 1995 Mudbanks of SW coast of India II: Wave-Mud interaction; *J. Coast. Res.* **11** 178–187
- McLellan T N, Pope M K and Burke C E 1990 Benefits of nearshore placement. Proc. Third Ann. Nat. Beach Preser. Tech. Conf, Florida Shore and Beach Preservation Assoc., Tallahassee, 339–353
- Mehta A J and Jiang F 1993 Some observations on water wave attenuation over nearshore underwater mudbanks and mud berms; *Tech. Rep. Coastal and Ocean. Engg. Dept. UFL/COEL/MP-93/01*, Univ. of Florida, Gainesville, Florida 45 pp
- Nair R R 1976 Unique mudbanks, Kerala, south west India; *Amer. Assoc. Pet. Geol.* **60(4)** 616–621
- Nair P V R, Gopinathan C P, Balachandran V K, Mathew K J, Reghunathan A, Rao D S and Murthy A V S 1984 Ecology of mudbanks Phytoplankton productivity in Alleppey mudbank; *CMFRI Bulletin* **31** 28–34
- Nair A S K 1985 Morphological variation of mudbank and their impact on shoreline stability; *Proc. Coastal and Ocean Engg. (Australian) Conf.* **2** 468–479
- Oltman-Shay J, Howd P A and Birkemeir W A 1989 Shear instabilities of the mean longshore current: (2). Field Observations; *J. Geophys. Res.* **94(C12)** 18031–18042
- Putrevu U and Svendsen Ib A 1992 Shear instability of longshore currents: A numerical study; *J. Geophys. Res.* **97(C5)** 7283–7303
- Putrevu U and Svendsen Ib A 1993 Vertical structure of undertow outside the surf zone; *J. Geophys. Res.* **98(C12)** 22707–22717
- Rao D S, Mathew K J, Gopinathan C P, Reghunathan A and Murthy A V S 1984 *CMFRI Bulletin* **31** 25–27
- Silas E G 1984 Mudbanks of Kerala-Karnataka – Need for an integrated study; *CMFRI Bulletin* **31** 2–7
- Silvester R 1977 The role of wave reflections in coastal processes; *Proc. Coastal Sediments* **77** 639–654
- Tatavarti V S N Rao 1989 The reflection of waves on natural beaches; *Ph.D Thesis*, Dalhousie Univ., Canada, 175 pp
- Tatavarti V S N Rao and Bowen A J 1989 Mean currents and undertow in the nearshore zone: Observations from C-COAST experiments. *Proc. Workshop on C-COAST*, Univ. of Toronto, Canada
- Tatavarti R, Narayana A C, Manoj Kumar P and Ravishankar M 1996. Mudbank Dynamics: Field evidence of edge waves and FIG waves; *Current Science* **70** 837–843
- Thompson P K R 1986 Seasonal distribution of cyclopoid copepods of the mudbanks off Allepey, Kerala coast; *J. Mar. Biol. Assoc.* **28(1 & 2)** 48–56
- Wells J T and Coleman J M 1981 Periodic mudflat progradation, Northeastern coast of South Africa; *J. Sed. Petrol* **51(4)** 1069–1075
- Wells J T and Kemp G P 1986 Interaction of surface waves and cohesive sediment: Field observations and geologic significance. In: *Estuarine Cohesive Sediment Dynamics*, (ed.) A J Mehta (New York: Springer-Verlag) 43–65